Anqing Xing[1] *and Delwyn G. Fredlund*[2]

Numerical Modeling of a Thermal Conductivity Matric Suction Sensor

Authorized Reprint from Geotechnical Testing Journal Dec. 1994
Copyright 1995 American Society for Testing and Materials, 1916 Race Street, Philadelphia, PA 19103

REFERENCE: Xing, A. and Fredlund, D. G., **"Numerical Modeling of a Thermal Conductivity Matric Suction Sensor,"** *Geotechnical Testing Journal*, GTJODJ, Vol. 17, No. 4, December 1994, pp. 415–424.

ABSTRACT: Thermal conductivity matric suction sensors appear to be a promising device for the measurement of suction in soil. The technique indirectly measures matric suction by measuring the thermal conductivity of a ceramic block. This paper uses both a spherical and a cylindrical porous medium to simulate the heat flow in a thermal conductivity matric suction sensor. It is found that, although the transient temperature at the center of the sensor is heavily dependent on the material of the thermocouple and the heating device, the steady-state temperature is primarily determined by the thermal conductivity of the ceramic block. Therefore, accurate measurements can be obtained by using a longer heating period or by selecting a lower-heat-capacity material for the thermocouple and the heating device. Optimal sizes of the sensor for given heating rates and heating periods are calculated using a finite difference method. A multilayered sphere was also used to simulate the situation where the size of the sensor is not sufficiently large and an error occurs due to the influence of the surrounding soil. The numerical model is verified by comparison with the theoretical solution of a special case.

KEYWORDS: numerical modeling, matric suction sensor, thermal conductivity, optimal size

Matric suction is one of the stress state variables used to describe the behavior of unsaturated soils. The development of techniques and devices for measuring matric suction is important to the advancement of soil mechanics for unsaturated soils. Of particular need is a device that measures matric suction in situ.

A thermal conductivity matric suction sensor consists of a thermocouple and a heating device embedded in a standard porous ceramic block. A comprehensive study of the performance of thermal conductivity sensors was conducted by Fredlund (1990). The detailed design and data acquisition for the sensor was given by Gan et al. (1994). The sensor can be inserted into the soil and left to equilibrate until the matric suction in the ceramic is the same as the matric suction in the soil. When equilibrium is established, the matric suction of the soil can be determined by measuring the thermal conductivity of the standard ceramic block.

The sensor is first heated at a standard rate for a fixed heating period. During the heating period, part of the heat is dissipated, and the undissipated heat results in a temperature increase at the center of the ceramic block. The amount of heat dissipation is controlled by the presence of water in the ceramic block since water is a better thermal conductor than air. The water content of the ceramic block is dependent upon the matric suction applied to the ceramic block by the surrounding soil. Thus, the change in the thermal conductivity of the ceramic block is closely related to the change in matric suction of the surrounding soil. In other words, the temperature increase at the center of the sensor due to the heat pulse is a function of the matric suction of the surrounding soil being tested.

The ratio of the thermal conductivity of the ceramic block when saturated to that when it is dry gives an indication of the precision with which its water content can be measured by the thermal conductivity method. Ideally, this ratio, or the void ratio of the ceramic block, should be as great as possible. Equally important is the pore-size distribution of the ceramic block. A variety of pore sizes are needed to measure a suitable range of matric suction values. The pore-size distribution of the ceramic block is a significant characteristic since it governs the sensor response and sensitivity to changes in matric suction.

The size of the sensor should be as small as possible to expedite equilibrium. However, the ceramic block must be sufficiently large to contain the heat pulse. Otherwise, the readings from the sensor will be influenced by the thermal properties of both the ceramic block and the surrounding soil. The optimum size of the sensor depends on heating rate and heating period. Theoretically, if the heating period and heating rate are fixed, the optimal size of the sensor can be determined. Conversely, if the size of the sensor and heating rate are given, the maximum heating period can be determined. This paper uses a spherical model to determine the optimal sizes for different combinations of heating rate and heating period.

Spherical Mathematical Model and Numerical Solution

An infinite sphere with radius r ($0 < r < \infty$) is first used as a model to determine the optimal size of the sensor for a fixed heating period and heating rate. The region of the sphere, $0 < r < a$, the inner sphere, contains the thermocouple and the heating device, and the region, $r \geq a$, is the infinite porous medium (Fig. 1). From Table 1, it can be inferred that the thermal conductivity of a porous medium is at a maximum when the porous medium is saturated. Of the potential materials for porous block, gypsum has the highest saturated thermal diffusivity (Table 1). Therefore, the radius determined for saturated gypsum should be sufficient to contain the heat pulse for any of the other material listed in

[1]Research fellow, Department of Civil Engineering, University of Saskatchewan, Saskatoon, Saskatchewan S7N 0W0.
[2]Head, Department of Civil Engineering, University of Saskatchewan, Saskatoon, Saskatchewan S7N 0W0.

© 1994 by the American Society for Testing and Materials

TABLE 1—*Thermal conductivity, thermal diffusivity and percent pore space for porous material considered for matric suction sensors (after Phene at al. 1971).*

Material	Thermal Conductivity, λ (W/m · K)		Thermal Diffusivity, D ($\times 10^{-6}$ m^2/s)		Ratio		Porosity, n (%)
	Air Dry	Wet	Air Dry	Wet	λ (wet) / λ (dry)	D (wet) / D (dry)	
Ceramic	0.476976	0.769856	0.1180	0.3830	1.62	3.25	17.8
Refined ceramic	0.364008	0.673624	0.1310	0.1690	1.85	4.73	25.6
Caston and ground ceramic	0.506264	1.146416	0.0680	0.3330	2.26	4.9	28.4
Gypsum	0.317984	0.803328	0.1010	0.5100	2.53	5.05	44.5
Water		0.602496		0.1440			
Air	0.024267		18.7000				

Table 1. For this reason, the infinite porous medium, $r \geq a$, is assumed to be made of saturated gypsum.

The radial heat conduction equation for an infinite medium, when expressed in spherical polar coordinates, is (Carslaw and Jaeger, 1959)

$$\frac{\partial T}{\partial t} = D\left(\frac{\partial^2 T}{\partial r^2} + \frac{2}{r}\frac{\partial T}{\partial r}\right) \tag{1}$$

where

T = $T(t, r)$ is the temperature (K) in the sphere at time t and radius r,
D = thermal diffusivity (m^2/s) of the porous medium, and $t \geq 0$ and $r \geq a$.

The thermal conductivity and thermal diffusivity of the porous medium can be assumed to be constant within the temperature range of the sensor. Therefore, the temperature increase is independent of the initial temperature, and a zero initial temperature (i.e., 0°C or 273.15 K) in the sphere is assumed for the purpose of mathematical treatment. That is, $T(0, r)$ is equal to 273.15 for $0 < r < \infty$. When heat is generated at the center of the sphere for a period of time, t_p, there will be a temperature increase in the area near the center of the sphere (i.e., $T(t_p, r) > 273.15$ for small values of r, and the temperature, $T(t_p, r)$, becomes 273.15 as r increases). Since radial heat flow is being considered, there is a radius, R, beyond which the temperature increase is less than a given error tolerance, e. In this case, the radius, R, is considered the optimal radius. This implies that any point with r greater than R is assumed to not be affected by the heat pulse. The maximum heating period for a given sensor size and heating rate can be determined similarly.

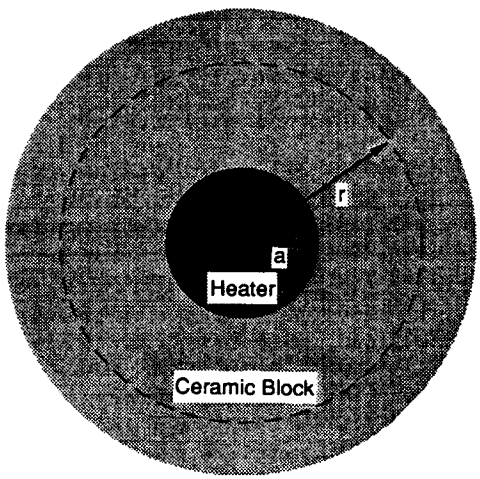

FIG. 1—*Cross-section of the spherical model used for the thermal conductivity matric suction sensor study.*

Since the thermal conductivity of the inner sphere, $0 < r < a$, is much higher than that of the porous medium, it can be assumed that the inner sphere is a perfect conductor. Let us also assume that there is no contact resistance at the surface, $r = a$. Some of the heat generated in the inner sphere is dissipated. The undissipated heat results in a temperature increase in the inner sphere. Let Q denote the heating rate (W) generated in the inner sphere. The amount of heat generated in a small time interval, dt, is Qdt. By Fourier's law, the amount of dissipated heat, H_1, in the small time interval, dt, is

$$H_1 = -\lambda 4\pi a^2 \frac{\partial T}{\partial r} dt \tag{2}$$

where

λ = thermal conductivity of the porous medium (W/m · K).

Let V be the temperature of the inner sphere. Since the inner sphere is assumed to be a perfect conductor, V is a function of time, t, and is independent of the spatial distance, r. If dV is the increase of the temperature of the inner sphere in the small time interval, dt, the amount of undissipated heat, H_2, is

$$H_2 = \frac{4}{3}\pi a^3 \rho c dV \tag{3}$$

where

ρ = density of the inner sphere (kg/m^3), and
c = specific heat of the inner sphere (J/kg · K).

The total amount of heat generated in the inner sphere is equal to the dissipated heat (i.e., H_1) plus the undissipated heat (i.e., H_2). That is,

$$Qdt = \frac{4}{3}\pi a^3 \rho c dV - 4\pi a^2 \lambda \frac{\partial T}{\partial r} dt \tag{4}$$

Dividing both sides of Eq 4 by dt gives the following boundary condition at $r = a$.

$$Q = \frac{4}{3}\pi a^3 \rho c \frac{dV}{dt} - 4\pi a^2 \lambda \frac{\partial T}{\partial r} \quad (5)$$

From the assumption that there is no contact resistance at $r = a$, it follows that $V = T$ at $r = a$ and Eq 5 becomes

$$Q = \frac{4}{3}\pi a^3 \rho c \frac{\partial T}{\partial t} - 4\pi a^2 \lambda \frac{\partial T}{\partial r} \quad (6)$$

As mentioned previously, the initial condition can be assumed to be 273.15 K (i.e., 0°C) without any loss in generality. Let $T(t, r)$ be a solution of Eq 1 with the boundary condition given by Eq 6 and with an initial temperature of 273.15 K. It can be easily verified that $T(t, r) - 273.15 + T_0$ satisfies Eqs 1 and 6 and, therefore, is a solution of Eq 1 with the boundary condition given by Eq 6, but with the initial temperature, T_0.

Equations 1 and 6 can be solved using the explicit finite difference method as follows. From Eq 1, we have

$$\frac{T_{i+1,j} - T_{i,j}}{\Delta t} = D\left(\frac{T_{i,j+1} - 2T_{i,j} + T_{i,j-1}}{\Delta r^2} + \frac{2}{a + j\Delta r}\frac{T_{i,j} - T_{i,j-1}}{\Delta r}\right) \quad (7)$$

where

$i = 0, 1, 2, \ldots$
$j = 1, 2, \ldots$
Δt = length of the time step, and
Δr = length of the radius step.

From Eq 6, it follows that

$$Q = \frac{4}{3}\pi a^3 \rho c \frac{T_{i+1,0} - T_{i,0}}{\Delta t} - 4\pi a^2 \lambda \frac{T_{i+1,1} - T_{i+1,0}}{\Delta r} \quad (8)$$

where

$i = 0, 1, 2, \ldots$

Rearranging Eq 7 gives

$$T_{i+1,j} = T_{i,j} + \frac{D\Delta t}{\Delta r^2}\left(T_{i,j+1} - 2T_{i,j} + T_{i,j-1} + \frac{2}{a/\Delta r + j}(T_{i,j} - T_{i,j-1})\right) \quad (9)$$

Solving for the temperature at the contact surface from Eq 8 gives

$$T_{i+1,0} = \frac{\Delta r \Delta t Q}{\alpha} + \frac{\frac{4}{3}\pi a^3 \rho c \Delta r}{\alpha} T_{i,0} + \frac{4\pi a^2 \lambda \Delta t}{\alpha} T_{i+1,1} \quad (10)$$

where

$$\alpha = \frac{4}{3}\pi a^3 \rho c \Delta r + 4\pi a^2 \lambda \Delta t$$

The initial temperature of 273.15 K gives

$$T_{0,0} = T_{0,1} = T_{0,2} = T_{0,3} = \cdots = 273.15 \quad (11)$$

From Eq 9 it can be seen that $T_{i+1,j}$ is evaluated in terms of the three known or previous values of T at nodes (i, j), $(i, j - 1)$ and $(i, j + 1)$. The solution can proceed in a recursive manner by computing the temperature over the spatial domain for future times after the initial values have been established. It should be noted that, in order to get a stable solution, the ratio $D\Delta t/\Delta r^2$ in Eq 9 must be less than or equal to 0.5 (Wang and Anderson 1982).

Results of the Numerical Analysis on the Spherical Model

A computer program was written, based on the finite difference technique, to calculate the temperature, $T_{i,j}$, radiating within a sphere. The values of the parameters used in the model are presented in Table 2. The results for a heat source with Q equal to 8.368×10^{-3} W, 4.184×10^{-2} W, and 0.1 W are shown in Figs. 2 to 4. The heating period is assumed to be 60 s in all the cases. Figure 2 shows the temperatures at the center of the sphere as a function of time for different heating rates. After a heating period of 60 s, the temperatures as a function of radius for different heating rates are shown in Fig. 3. For Q equal to 0.1 W, Fig. 4 shows the temperature distributions in the sphere at different times during the heating period of 60 s. The optimal radii for a sensor for different heating rates and different heating periods are presented in Table 3.

When the inner sphere is continuously heated at a given heating rate, its temperature increases rapidly during the first part of the heating period (i.e., the transient period). As the temperature continues to increase, the temperature gradient, $\partial T/\partial r$, at the surface of the inner sphere also increases, resulting in more heat being dissipated. Eventually, a steady-state temperature is approached. When the inner sphere reaches its steady-state temperature, the temperature gradient at the surface of the inner sphere reaches a maximum value under which all the generated heat is dissipated. This steady-state temperature is primarily determined by the thermal conductivity, λ, of the porous medium and is not affected by the material of the inner sphere. The material of the inner sphere affects its temperature only during the transient period. For the same heating rate and the same radius for the inner sphere, Fig. 5 shows the temperatures of the inner sphere made of copper and tin, respectively. As shown in Fig. 5, the two curves differ during the first 2 min and are essentially the same after the transient period.

The size of the inner sphere is another factor which affects the temperature at the center of the sphere. For the same heating period and the same material for the inner sphere, Fig. 6 shows the temperatures for different radii for the inner sphere.

As shown by the results, the temperature in the inner sphere during the transient period is controlled mainly by the thermal

TABLE 2—*Values of the parameters used in the model.*

Variable	Unit	Assumed Value
Thermal conductivity of saturated gypsum, λ	W/m · K	0.803328
Thermal diffusivity of saturated gypsum, D	$\times 10^{-6}$ m^2/s	0.51
Radius of the inner sphere (thermocouple and heater), a	$\times 10^{-2}$ m	0.3
Density of the material (copper) for the inner sphere, ρ	kg/m^3	8.94
Specific heat of the material (copper) for the inner sphere, c	J/kg · K	382.4176
Length of the time step, Δt	s	0.02
Length of the radius step, Δr	$\times 10^{-2}$ m	0.02
Error tolerance, e	K	0.01

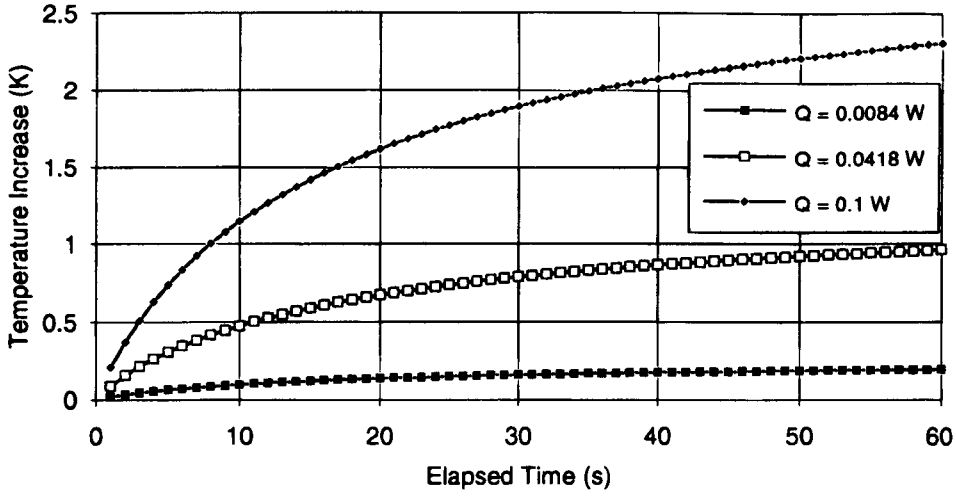

FIG. 2—*Temperature versus elapsed time in the inner sphere for different heating rates.*

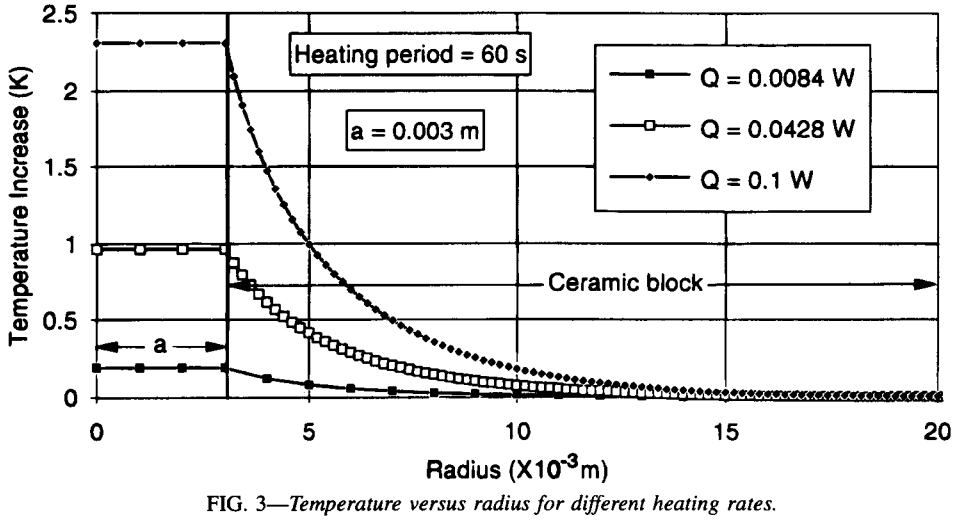

FIG. 3—*Temperature versus radius for different heating rates.*

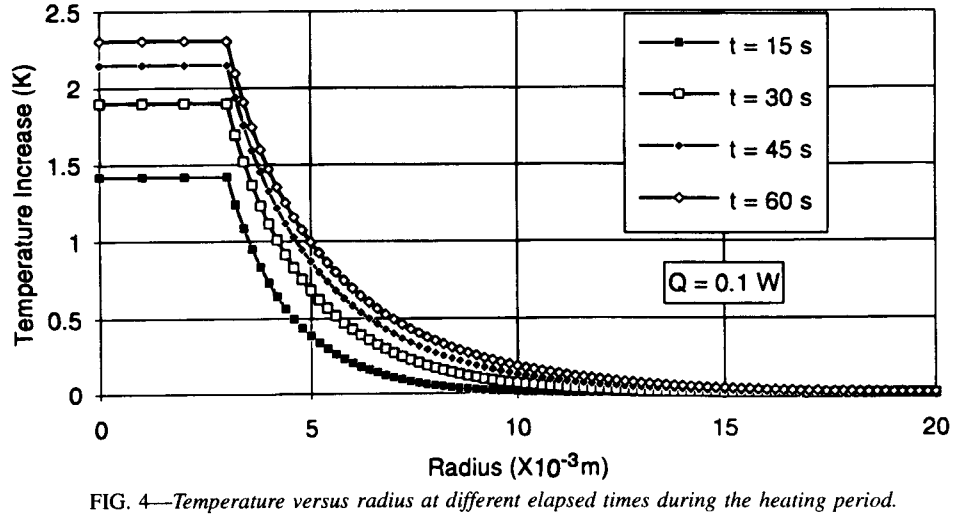

FIG. 4—*Temperature versus radius at different elapsed times during the heating period.*

TABLE 3—*Minimum sensor radius for different heating rates and different heating periods.*

Heating rate, W	Minimum Sensor Radius ($\times 10^{-2}$ m) for Different Heating Periods, s						
	60	90	120	150	180	210	240
0.004184	0.92	1.06	1.16	1.24	1.32	1.38	1.42
0.008368	1.14	1.32	1.46	1.58	1.68	1.78	1.86
0.012552	1.26	1.46	1.64	1.78	1.90	2.00	2.10
0.016736	1.34	1.58	1.76	1.90	2.04	2.16	2.28
0.020920	1.40	1.64	1.84	2.02	2.16	2.28	2.40
0.025104	1.46	1.72	1.92	2.10	2.26	2.38	2.52
0.029288	1.50	1.76	1.98	2.16	2.32	2.48	2.60
0.033472	1.54	1.82	2.04	2.22	2.40	2.54	2.68
0.037656	1.56	1.86	2.08	2.28	2.46	2.60	2.74
0.041840	1.60	1.88	2.12	2.32	2.50	2.66	2.80
0.046024	1.62	1.92	2.16	2.36	2.52	2.72	2.86
0.050208	1.64	1.94	2.20	2.40	2.58	2.76	2.90
0.054392	1.66	1.98	2.22	2.44	2.62	2.80	2.96
0.058576	1.68	2.00	2.26	2.46	2.66	2.84	3.00
0.062760	1.70	2.02	2.28	2.50	2.70	2.88	3.04
0.066944	1.72	2.04	2.30	2.52	2.72	2.90	3.06
0.071128	1.74	2.06	2.32	2.56	2.76	2.94	3.10
0.075312	1.76	2.08	2.34	2.58	2.78	2.96	3.12
0.079496	1.76	2.10	2.36	2.60	2.80	2.98	3.16
0.083680	1.78	2.12	2.38	2.62	2.82	3.02	3.18
0.087864	1.80	2.12	2.40	2.64	2.86	3.04	3.20
0.092048	1.80	2.14	2.42	2.66	2.88	3.06	3.24
0.096232	1.82	2.16	2.44	2.68	2.90	3.08	3.26
0.100416	1.82	2.16	2.46	2.70	2.92	3.10	3.28

properties of the inner sphere. The steady-state temperature at the center of the sphere is determined by the thermal properties of the porous medium. Therefore, a longer heating period will produce a more accurate measurement of the thermal properties of the porous medium (and, in turn, the matric suctions of the surrounding soil). In other words, to increase the precision of the sensor, a longer heating period could be used. On the other hand, the sensor should be sufficiently large to contain the heat pulse. A longer heating period would require a larger sensor size.

As mentioned earlier, the size of the sensor should be as small as possible to expedite equilibrium. One way to keep the sensor size small is to reduce the heating rate. As shown in Table 3, the minimum radius of the sensor for Q equal to 8.368×10^{-3} W and a heating period of 240 s is 18.6×10^{-3} m. The minimum radius for Q equal to 0.1 W and a heating period of 60 s is 18.2×10^{-3} m. Another way to keep the sensor size small is to shorten the transient period. This can be achieved by selecting a material with a lower heat capacity for the thermocouple and the heating device. For a heating rate Q of 0.1 W, the temperature of the inner sphere during and after a heating period of 60 s is shown in Fig. 7.

Phene et al. (1971) used a finite spherical model to calculate the optimal size of a sensor. Their model was a sphere of radius, b, which contained a heater and a diode (made of germanium) in an inner sphere of radius, a, at the center ($a < b$). It was assumed that there was no contact resistance at the interface between the inner sphere and the porous medium. The temperature at the surface (i.e., $r = b$) was kept at 0°C (i.e., 273.15 K). For a fixed heating period and a fixed heating rate, the temperature at the center of the sensor increased with the radius of the sensor, as shown in Fig. 8. Any sensor whose temperature at its center after a heat pulse differed from that of an infinite sphere by less than 0.002 K was considered sufficiently large to contain the heat pulse. The points in Fig. 8 correspond to those radii beyond which the temperature does not change significantly. In addition, these points

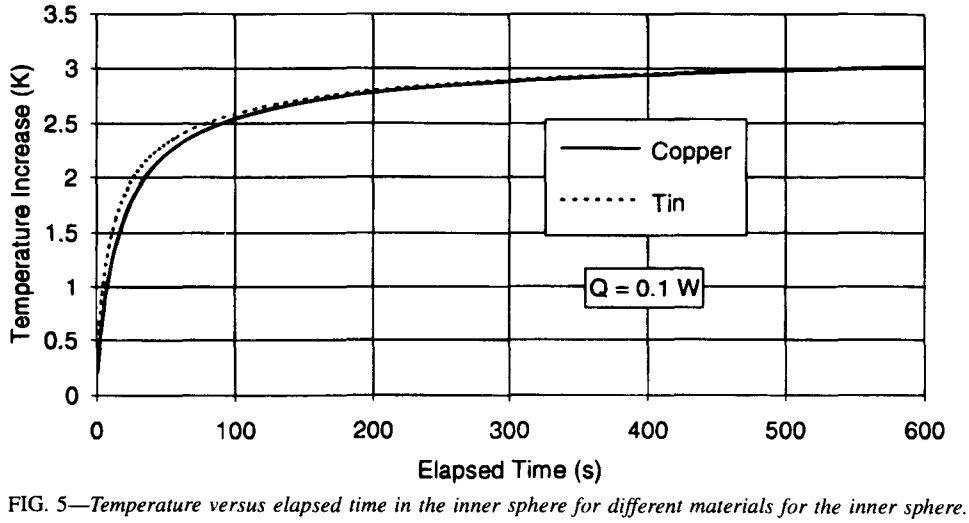

FIG. 5—*Temperature versus elapsed time in the inner sphere for different materials for the inner sphere.*

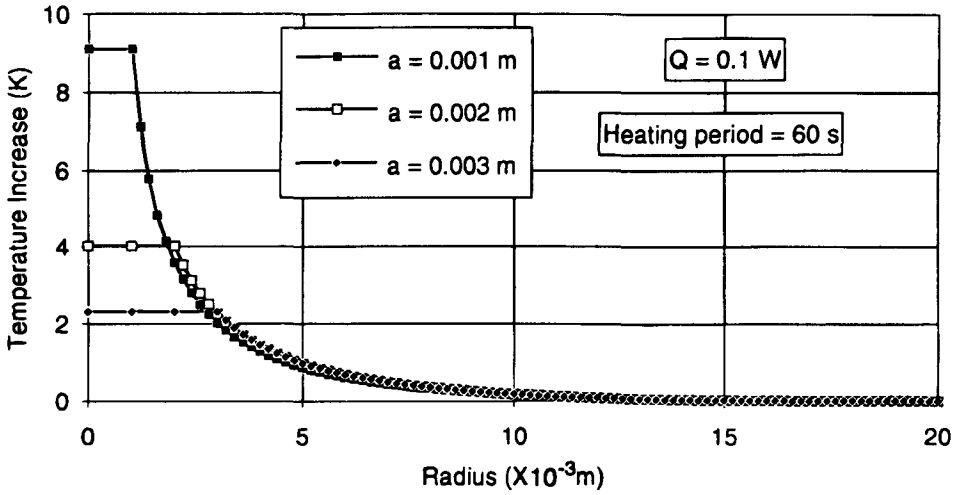

FIG. 6—*Temperature versus radius for different sizes of the inner sphere.*

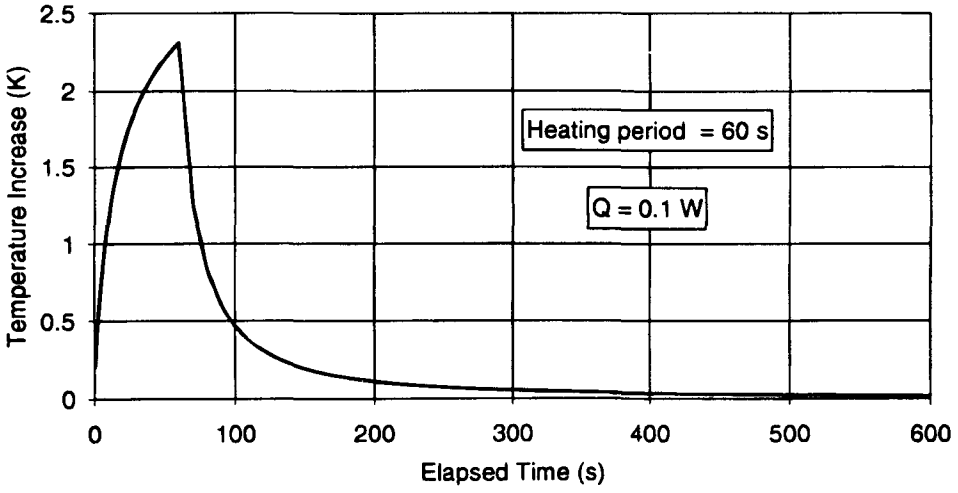

FIG. 7—*Temperature versus elapsed time in the inner sphere during and after the heating period.*

satisfy the above criteria and, therefore, were considered the minimum radii. Their results were based on the closed form solution given by Carslaw and Jaeger (1959) with a heating rate of 0.002 cal/s (i.e., 8.368×10^{-3} W). In order to compare their results with the finite difference solution, it is assumed that the inner sphere is made of germanium ($\rho = 5.31456$ kg/m^3 and $c = 359.8$ J/kg · K). The optimal sizes obtained by the finite difference model in this paper (i.e., for $a = 4 \times 10^{-3}$ m and $Q = 8.368 \times 10^{-3}$ W) are listed in Table 4. These results are close to those shown in Fig. 8 obtained by Phene at al. (1971). Note that the results in Table 4 are based on a spherical model of finite size.

A modification of the infinite sphere was used to simulate an infinite cylinder with an internal cylinder with a radius a at the center. Suppose that there is no contact resistance at the surface of the inner cylinder and heat is generated at the inner cylinder at a rate of Q per unit length. The heat conduction equation is (Carslaw and Jaeger, 1959)

$$\frac{\partial T}{\partial t} = D\left(\frac{\partial^2 T}{\partial r^2} + \frac{1}{r}\frac{\partial T}{\partial r}\right) \tag{12}$$

and the boundary condition at the surface of the inner cylinder can be similarly obtained as

$$Q = \pi a^2 \rho c \frac{dT}{dt} - 2\pi a \lambda \frac{\partial T}{\partial r} \tag{13}$$

For the same heating rate (i.e., $Q = 0.1$ W) comparable temperatures for the two cases are shown in Fig. 9. It can be seen that the optimal size for a cylinder is larger than that for the sphere.

As mentioned above, the sensor must be sufficiently large to contain the heat pulse. Otherwise, the reading of the sensor will be influenced by the surrounding soil. Suppose that the sensor is a sphere with a radius of 0.01 m and is surrounded by a soil with a thermal conductivity, λ_s. The inner sphere at the center of the sensor has a radius of 0.003 m. Figure 10 shows the temperature distribution in the sensor and the surrounding soil for $\lambda_s > \lambda$, $\lambda_s < \lambda$, and $\lambda_s = \lambda$, where λ is the thermal conductivity of the ceramic block. The heating period is 60 s and Q is equal to 0.1 W. It can be seen that, if the thermal conductivity of the soil is different from that of the porous block, a different temperature reading at the center of the sensor results.

Let us assume that the thermal conductivity of the surrounding soil, λ_s, is infinite. This gives rise to the maximum measurement error possible at the center of the sensor, which can be caused by the surrounding soil. The results show that, for the most commonly used sensors which have a radius of 0.01 m, the maximum measure-

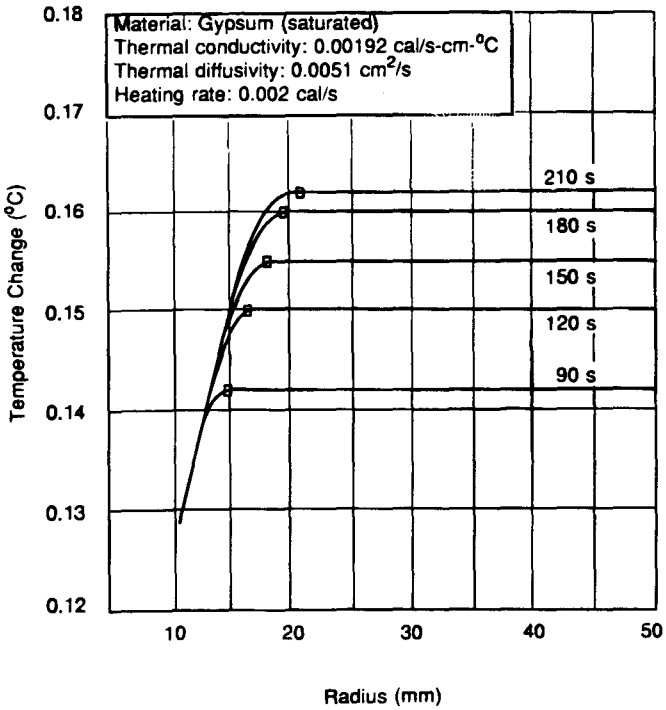

FIG. 8—*Temperature increase of diode as a function of sensor radius for various heating periods (after Phene et al. 1971).*

TABLE 4—*Optimal sizes based on the model of finite sphere.*

Heating period, s	Optimal Radius, × 10^{-2} m
90	1.44
120	1.62
150	1.78
180	1.92
210	2.04

ment error at the center of the sensor caused by the surrounding soil is 0.0689 K. Based on the steepest calibration curve available, the maximum measurement error is about 78 kPa in terms of matric suction. The actual error would be much smaller since this error is calculated for the worst possible case. In reality, less heat is dissipated since the thermal conductivity of ceramic is lower than that of saturated gypsum and there is always a contact resistance between the inner sphere and the ceramic block. The thermal conductivity of the surrounding soil, λ_s, is usually close to that of the ceramic. Therefore, the effect of the surrounding soil on the measurement is much smaller than the theoretical results calculated for the worst case. Furthermore, some of the error is eliminated during the calibration process. The calibration of thermal conductivity sensors are performed by applying a range of matric suction values to the sensors while they are mounted in a soil. Readings of the change in temperature output from the sensor are taken at each applied suction value. The change in temperature output is a measure of the thermal conductivity (or water content) of the porous block under the applied suction. If the soil used for calibration and the soil being tested in the field have similar thermal properties and all other conditions are the same, the resulting error in the measurement would be very small.

A Special Case Analytical Solution

Performing the Laplace transforms on both sides of Eq 1 gives

$$p\bar{T} = D\left(\frac{d^2\bar{T}}{dr^2} + \frac{2}{r}\frac{d\bar{T}}{dr}\right) \tag{14}$$

which can also be written as

$$\frac{d^2(r\bar{T})}{dr^2} - q^2(r\bar{T}) = 0 \tag{15}$$

where

$q^2 = p/D$,
$\bar{T} = \bar{T}(p, r)$, the Laplace transform of $T(t, r)$,
p = frequency domain variable corresponding to time t.

The boundary condition shown in Eq 6 becomes

$$\frac{Q}{p} = \frac{4}{3}\pi a^3 \rho c p \bar{T} - 4\pi a^2 \lambda \frac{d\bar{T}}{dr} \tag{16}$$

Equation 15 is a second-order ordinary differential equation with a boundary condition given by Eq 16. Its solution can be obtained as

$$\bar{T}(p, r) = \frac{Qa}{p[(4/3)\pi a^3 \rho c p + 4\pi a \lambda (aq + 1)]} \frac{e^{-q(r-a)}}{r} \tag{17}$$

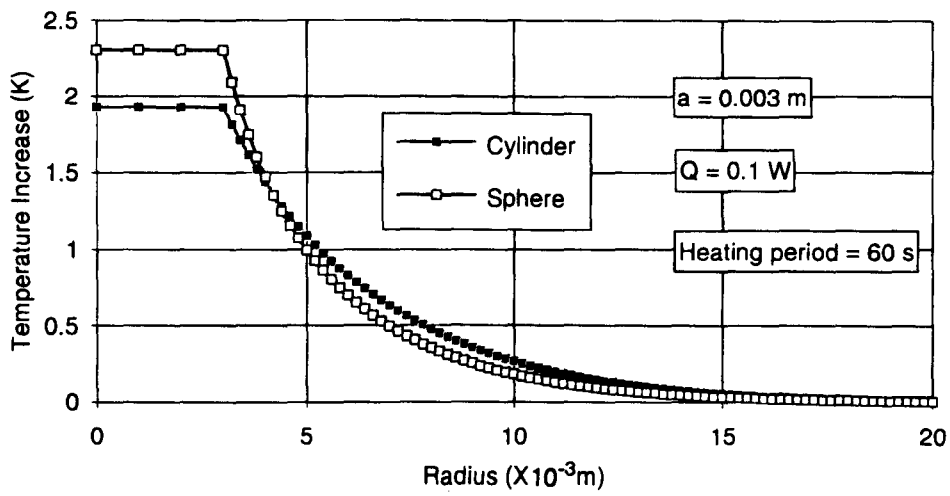

FIG. 9—*Comparison of the temperatures for a sphere and a cylinder.*

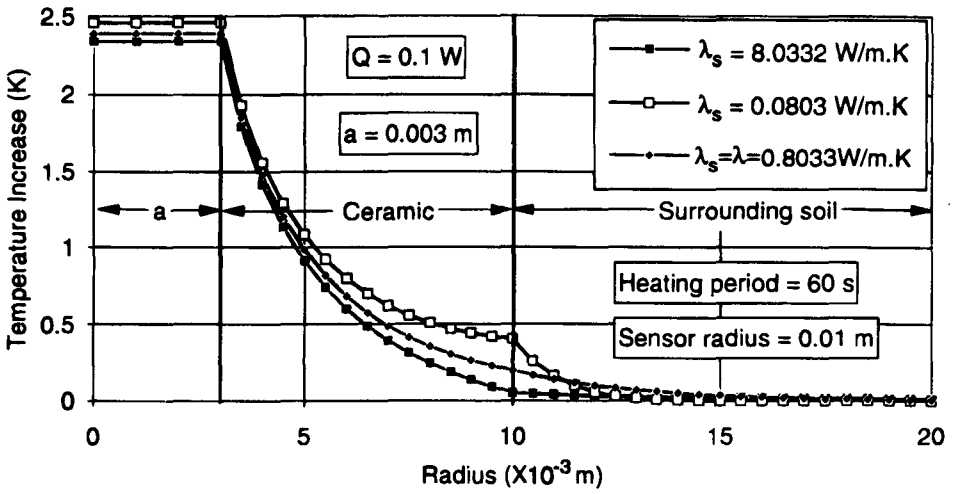

FIG. 10—*Temperature distributions in the sensor and the surrounding soil.*

For a special case, let us assume that the heat capacity of the inner sphere is equal to three quarters of the heat capacity of the porous medium

$$\rho c = \frac{3}{4}\frac{\lambda}{D} \tag{18}$$

Equation 17 becomes

$$\bar{T}(p, r) = \frac{Q}{4\pi r\lambda}\left[\frac{1}{p} - \frac{2}{\sqrt{p}\left(\sqrt{p} + \frac{2\sqrt{D}}{a}\right)} + \frac{1}{\left(\sqrt{p} + \frac{2\sqrt{D}}{a}\right)^2}\right] e^{-q(r-a)} \tag{19}$$

Performing the inverse Laplace transform on Eq 12 using Theorem XI given by Carslaw and Jaeger (1959)

$$T(t, r) = \frac{Q}{4\pi\lambda r}\left[erfc\left(\frac{r-a}{2\sqrt{Dt}}\right) - \frac{4}{a}\left(\frac{Dt}{\pi}\right)^{1/2} e^{\frac{-(r-a)^2}{4Dt}} + \left(\frac{2}{a}(r-a) + 8\frac{Dt}{a^2} - 1\right) e^{\frac{2(r-a)}{a} + \frac{4Dt}{a^2}} \times erfc\left(\frac{r-a}{2\sqrt{Dt}} + \frac{2\sqrt{Dt}}{a}\right)\right] \tag{20}$$

where

$$erfc(x) = \frac{2}{\sqrt{\pi}}\int_x^\infty e^{-s^2} ds = 1 - erf(x) = 1 - \frac{2}{\sqrt{\pi}}\int_0^x e^{-s^2} ds$$

The temperature of the inner sphere is given by setting $r = a$ in Eq 20. Therefore, the temperature at the center of the sphere as a function of time is

$$T(t, a) = \frac{Q}{4\pi a\lambda}\left[1 - \frac{4}{a\sqrt{\pi}}\sqrt{Dt} + \left(8\frac{Dt}{a^2} - 1\right) e^{4\frac{Dt}{a^2}} erfc\left(\frac{2\sqrt{Dt}}{a}\right)\right] \tag{21}$$

An approximation of Eq 21 can be made for small and large values of time as follows (Carslaw and Jaeger 1959). For the case where x is small

$$erf(x) = \frac{2}{\sqrt{\pi}}\sum_{n=0}^{\infty}\frac{(-1)^n x^{2n+1}}{(2n+1)n!} \tag{22}$$

For the case where x is large

$$erfc(x) = \frac{e^{-x^2}}{\sqrt{\pi}}\left(\frac{1}{x} - \frac{1}{2x^3} + \frac{1\cdot 3}{2^2 x^5} - \frac{1\cdot 3\cdot 5}{2^3 x^7} + \cdots\right) \tag{23}$$

Within the first few seconds of the heating period, the temperature of the inner sphere is controlled mainly by the heat capacity of the material used for the inner sphere and the heating rate. For large values of time, the temperature of the inner sphere can be expressed as follows.

$$\frac{Q}{4\pi a\lambda}\left[1 - \frac{a}{\sqrt{\pi Dt}} + \frac{a^3}{4\sqrt{\pi}(Dt)^{3/2}} - \cdots\right] \tag{24}$$

For a heating rate of Q equal to 8.368×10^{-3} W, numerical values are obtained for the first 10 s and the last 5 min during a heating period of 10 min. These values are close to the finite difference solution shown in Fig. 11.

Backcalculation of Thermal Conductivity and Thermal Diffusivity of a Spherical Porous Medium

The temperature response of a matric suction sensor can be used to estimate the thermal conductivity and the thermal diffusivity of the ceramic block of the sensor. The theoretical temperature, $T(t, a)$, at the center of the sphere for large values of time can be approximated by the following equation.

$$T(t, a) = \frac{Q}{4\pi a\lambda}\left[1 - \frac{a}{\sqrt{\pi Dt}} + \frac{a^3}{4\sqrt{\pi}(Dt)^{3/2}} \times \left(2 - \frac{4}{3}\rho c\frac{D}{\lambda}\right) - \cdots\right] \tag{25}$$

This equation can be verified by performing the inverse Laplace transform on Eq 17. Using the first two terms from Eq 25, the

temperature at the center of the sphere for large values of time can be approximated by

$$T(t, a) = A - B\frac{1}{\sqrt{t}} \tag{26}$$

where

$$A = \frac{Q}{4\pi\lambda a}, \qquad B = \frac{Q}{4\pi\lambda\sqrt{\pi D}}$$

A and B can be determined by the measuring of temperature at two different times. Once A and B are known, the thermal conductivity, λ, is computed as

$$\lambda = \frac{Q}{a\pi aA} \tag{27}$$

With the thermal conductivity, λ, known, the thermal diffusivity, D, is determined as

$$D = \left(\frac{Q}{4\pi^{3/2}\lambda B}\right)^2 \tag{28}$$

For large values of t (i.e., $t > 60$ s), Eq 26 gives a good approximation to the actual temperature curve. Therefore, measurements should be taken after 60 s in order to obtain a good approximation of the thermal conductivity and thermal diffusivity of the porous medium.

If the density and the specific heat of the inner sphere are known, the first three (instead of the first two) terms in Eq 25 can be used to obtain more accurate results. In this case, the temperatures at three different times have to be taken.

Equation 26 indicates that, for large values of time (i.e., $t > 60$ s) after commencing the heating process, the temperature at the center of the sphere is a linear function of the inverse square root of time. Therefore, if the temperature at the center of the sphere is plotted as a function of the inverse square root of time, Eq 26 is simply a tangent line on the temperature curve for a large value

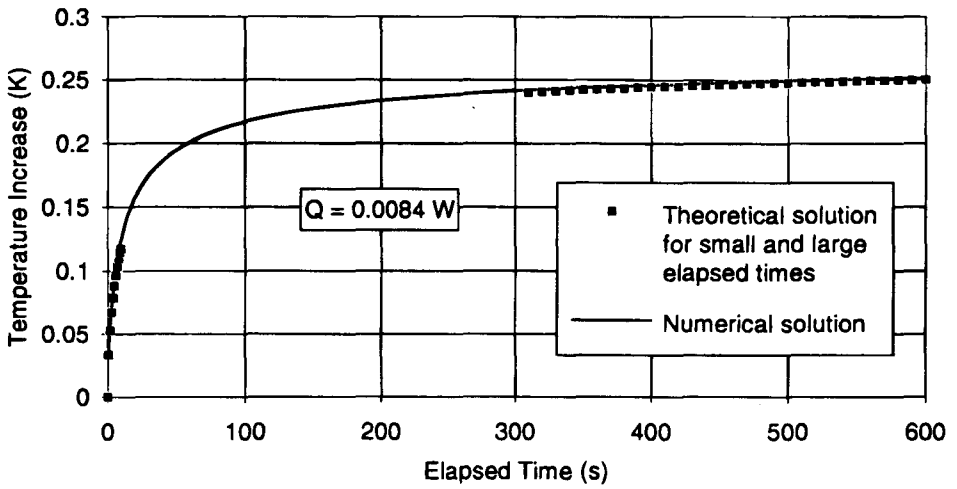

FIG. 11—*Comparison of the numerical solution with the theoretical solution for small and large values of elapsed time.*

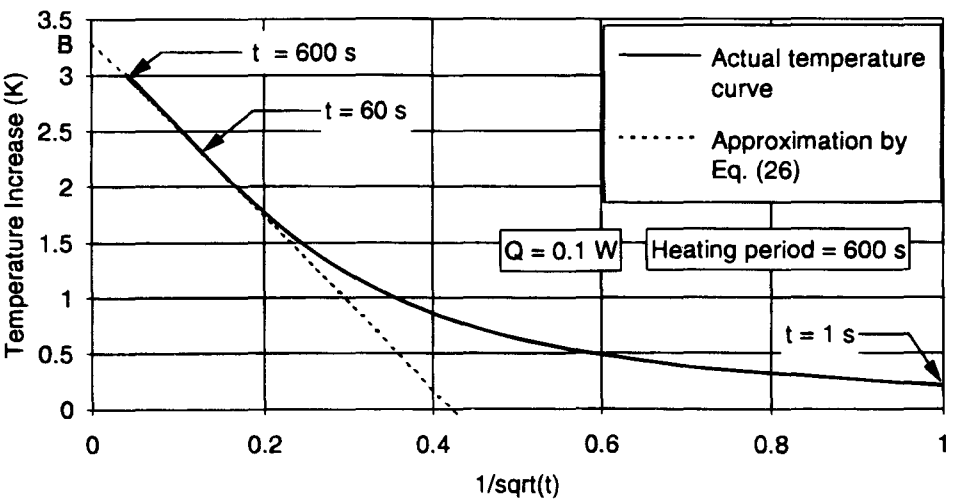

FIG. 12—*Temperature at the center of the sphere as a function of the inverse square root of time (for estimation of thermal conductivity, Eq 26 is approximated by a tangent line at the left end-point of the curve).*

of time (Fig. 12). An estimation for the thermal conductivity and the thermal diffusivity of the porous medium (i.e., the ceramic block) can be obtained using the slope and the intercept on the temperature axis of the tangent line for the values of B and A.

Conclusions

The thermal response characteristics of a porous medium were calculated using the thermal conductivity and thermal diffusivity of saturated gypsum, which are higher than those of many ceramics. It was assumed that there is no contact resistance between the heating device and the porous block. In the actual situation there is always a contact resistance between the heating device and the porous block, and the sensor is not always saturated. Therefore, if a sensor is made of ceramic, less heat will be dissipated when compared with the results obtained in this paper. This implies that the required optimal size of sensor, based on computations presented in this paper, is sufficient to contain the heat pulse for sensors made of ceramic.

The numerical results obtained in this paper are compared with those obtained by Phene (1971), where numerical evaluations were used to approximate a theoretical solution obtained by Carslaw and Jaeger (1959). The finite difference solution is close to the theoretical solution.

The accuracy of the sensor can be increased by using a longer heating period or by selecting a low-heat-capacity material for the thermocouple and the heating device. If a cylindrical sensor (with an inner cylinder containing a heating device and a thermocouple at the center) is to be designed with the same heating rate, the size of the sensor must be larger than if a spherical sensor is used. The finite difference solution was compared with a theoretical solution for a special case for small and large elapsed times.

This paper provides a general analysis of thermal conductivity sensors. Most of the numerical results are based on the model specifications listed in Table 2 (i.e., $a = 0.003$ m, material of the inner sphere = copper, and error tolerance = 0.01 K). For different specifications, or if the thermal properties of the actual ceramic block are available, this finite difference model can be used for design purposes.

References

Carslaw, H. S. and Jaeger, J. C., 1959, *Conduction of Heat in Solids,* 2nd ed., Oxford University Press, London, p. 510.

Fredlund, D. G., 1990, "Background, Theory and Research Related to the Use of Thermal Conductivity Sensors," *Proceedings,* Symposium on Measurement of Soil Physical Properties at the ASA, CSSA, SSSA Annual Meetings, San Antonio, TX.

Gan, J. K.-M., Fredlund, D. G., Xing, A., and Li, W.-X., 1994, "The Design and Data Acquisition for Thermal Conductivity Matric Suction Sensors," Transportation Research Board, 73rd Annual Meeting, Washington, DC.

Phene, C. J., Hoffman, G. J., and Rawlins, S. L., 1971, "Measuring Soil Matric Potential in Situ by Sensing Heat Dissipation With a Porous Body: Theory and Sensor Construction," *Soil Science Society of America Proceedings,* Vol. 35, pp. 27–32.

Wang, H. F. and Anderson, M. P., 1982, *Introduction to Groundwater Modelling—Finite Difference and Finite Element Method,* Freeman, San Francisco, CA, p. 237.